Title

Fisheries shocks provide an opportunity to reveal multiple recruitment sources of sardine in the Sea of Japan

Authors

Tatsuya Sakamoto[1*], Motomitsu Takahashi[1], Kotaro Shirai[2], Tomoya Aono[2, 3], Toyoho Ishimura[3, 4]

Affiliation

1. Fisheries Resource Research Institute, Japan Fisheries Research and Education Agency, Nagasaki, Japan
2. Atmosphere and Ocean Research Institute, The University of Tokyo, Chiba, Japan
3. Department of Chemistry and Material Engineering, National Institute of Technology, Ibaraki College, Ibaraki, Japan
4. Graduate School of Human and Environmental Studies, Kyoto University, Kyoto, Japan

*Corresponding author

Email: tatsfish@gmail.com

Address: Instituto Português do Mar e da Atmosfera

Rua Alfredo Magalhães Ramalho, 6 Algés 1495-006 Lisboa, Portugal

Acknowledgement

We thank Noriko Izumoto (Atmosphere and Ocean Research Institute, The University of Tokyo), Kakeru Ouchi, Akito Ikari, Takayoshi Matsuura, Ayaka Iwashita and Ayase Tomotsune (National Institute of Technology, Ibaraki College) for contributions to otolith isotope data collection. We appreciate Shoko Abe, Yousuke Igeta and Takashi Setou (Japan Fisheries Research and Education Agency) for providing the outputs of hydrodynamic models.

Author's contributions

TS, MT, TA and TI conceived the ideas of this research; TS designed the methodology; TS, KS, TA and TI collected the data; TS analysed the data and wrote the first draft; All authors contributed critically to revising the draft and gave final approval for publication.

Data availability

The newly obtained otolith isotope data will be accessible from Dryad repository (data will be submitted upon acceptance).

Conflict of interest

The authors declare no conflict of interest.

Abstract

1. Understanding the sources of recruits is essential for stock assessments of marine fish populations. In 2014 and 2019, schools of Japanese sardine in the Sea of Japan and the East China Sea (SJ-ECS), which arrive in Japanese coastal areas for spawning each spring were shockingly sparse. Abundances of eggs and juveniles also showed abrupt declines, suggesting that sardine reproduction in the SJ-ECS was severely limited during these years. However, in spring of 2015 and 2020 age-1 fish appeared as usual in the coastal areas, along with fish of other ages, challenging the current assumption that sardine in the system is a self-recruiting subpopulation.

2. To test the self-recruiting hypothesis, we analysed the stable oxygen and carbon isotopes ($\delta^{18}O$, $\delta^{13}C$) for otolith areas formed during the first spring and summer in otoliths of age-0 and age-1 sardines in 2010 and 2013–2015 year-classes captured in the SJ-ECS, as indices of temperature and metabolic trajectories.

3. Age-0 sardines generally showed a significant decrease in otolith $\delta^{18}O$ from spring to summer, reasonably reflecting seasonal warming in the SJ-ECS. However, the majority of age-1 captured in spring 2011, 2015 and 2016 showed non-decreasing profiles of otolith $\delta^{18}O$, suggesting that the age-0 off the Japanese coast were not the main source of recruitment. The $\delta^{18}O$ for summer thus indicates different migration groups: the “locals" growing up off the Japanese coast and the migrating “nonlocals".

4. The isotope ratios of the “nonlocals” overlapped with those of age-0 captured in the subarctic western North Pacific, suggesting that the “nonlocals” may be migrants from the Pacific, or perhaps an unsampled potential northward migration group in the SJ-ECS. Only in 2014 did the majority of age-1 consist of the “locals”, suggesting that the abrupt decline in catches was caused by the absence of the “nonlocals” and accompanying adults.

5. *Synthesis and applications*
   Our results highlight the significant uncertainty in the population structure assumed for the current stock assessment models for Japanese sardine. Concentrated investigations on recruitment processes to test and quantify the potential migration groups are recommended to improve the assessment model.

Keywords

Population structure; Sardine; Otolith; Stable isotopes; Migration; Recruitment; Source-sink dynamics

Introduction

Understanding the seasonal movements and origins of exploited marine fish is crucial for assessing population linkages and defining management unit (i.e. stock) boundaries. Biomass estimations often rely on the assumption that the unit consists of fish with uniform vital rates (e.g., growth, mortality), and that the available data (e.g., observed catch, abundance indices, size or age composition) reflect recruitment within the stock rather than immigration from neighbouring units (Cardin et al., 2019). Disregarding the mixing of recruits from different origins and life-history traits may therefore compromise the accuracy of population productivity estimates (Kerr et al., 2014; de Moor & Butterworth, 2015) and hinder downstream studies, e.g. on the causes of biomass fluctuations, which are needed for future projections.

Sardines (*Sardinops* and *Sardina* spp.), globally distributed in temperate regions (Checkley et al., 2017), play a key role in energy transfer from planktons to higher trophic levels in productive marine ecosystems (Cury et al., 2011) and are of great economic importance (Alder et al., 2008). The western North Pacific and its marginal seas support one of the largest sardine populations on earth (Japanese sardine *Sardinops sagax melanostictus*) (Checkley et al., 2017), with annual catch exceeding 5 million tonnes in the late 1980s (FAO, 2021). The population structure of Japanese sardine has been debated since at least the 1930s (Nakai, 1962). Some biological approaches have been applied to infer origins and movements of sardine, such as differences in the number of vertebrae (Amemiya & Abe, 1933) or mitochondrial DNA (Okazaki et al., 1996), which have generally failed to detect clear population structures. However, given the distribution of spawning grounds and the narrow straits separating the Sea of Japan and the North Pacific (Fig. 1a), current fisheries management assumes the existence of two semi-discrete subpopulations, the Tsushima Warm Current subpopulation distributed in the Sea of Japan and the adjacent East China Sea (hereafter the SJ-ECS) and the Pacific subpopulation in the western North Pacific (Fig. 1a), and treats them as management units.

These two sardine subpopulations are assumed to have their own main source of recruitment. Spawning grounds are formed from winter to spring in the inshore of the Kuroshio and Tsushima Warm Currents (Oozeki et al., 2007; Furuichi et al., 2020; Fig. 1a). During summer, larvae and juveniles are widely distributed off the Japanese coastal

areas and southern Sea of Japan near the spawning grounds (Nakai, 1962; Yasuda et al., 2021; Aono et al., 2024), and also in the offshore Kuroshio-Oyashio transition zone (Fig. 1a, Niino et al., 2020). Those that grew in coastal areas in the SJ-ECS are considered to be the main recruits of the Tsushima Warm Current subpopulation. Eggs and age-0 juveniles were hardly found off the North Korean or Russian coasts in the Sea of Japan during surveys and fisheries in the 1920s–30s and 1970s–80s (Nakai, 1962; Dudarev & Kenya, 1988). For the Pacific subpopulation, juveniles distributed in the Kuroshio-Oyashio transition zone in summer and migrating northwards to the subarctic region (Sakamoto et al., 2019) are considered to be the main source of recruitment in recent years (Niino et al., 2020). These recruits mature sexually at age 1 or 2 (Morimoto, 2010), and migrate to coastal areas for reproduction during winter to spring.

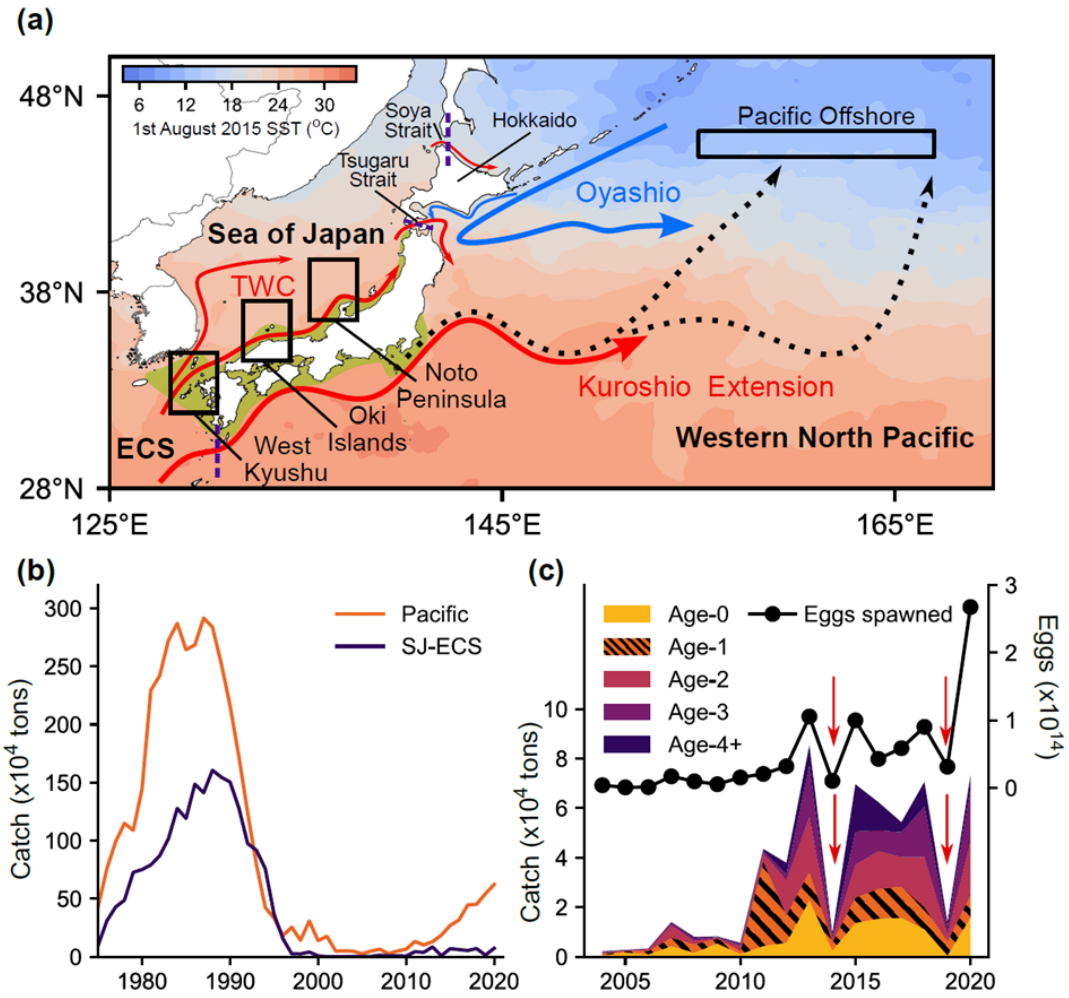

Figure 1. (a) Schematics of ocean currents around the distribution of Japanese sardine together with sample collection sites (black squares), spawning grounds (yellow shades) and satellite-based sea surface temperature on 1st August 2015. Red arrows show the typical positions of warmer currents originate from the subtropical Pacific and blue lines are those of cooler currents from subarctic regions. Black dotted lines the typical movement path of larvae and juveniles that use offshore nursery area in the Pacific. The three purple dashed lines show the boundaries of the currently assumed two subpopulations, namely the Tsushima Warm Current stock in the west and the Pacific stock in the east. (b) Long-term time series of Japanese fishery catch in the Pacific and SJ-ECS system. (c) Recent time series of egg abundance based on field surveys and catch of the sardine in the SJ-ECS system decomposed by age. The red arrows show the years of abrupt decline.

However, some observations in the SJ-ECS cannot be explained by the current hypothesis of population structure. Time series of fisheries catches in the SJ-ECS and the Pacific, which are assumed to be from semi-independent subpopulations, show similar decadal trends: both peak in the late 1980s, collapse in the 1990s and show signs of recovery in

the 2010s (Fig. 1b). Recent increases in sardine catch in the SJ-ECS began with the sudden appearance of age-1 fish in 2011, although few age-0 fish were caught in the system in 2010 (Fig. 1c). Coincidentally or not, an extremely strong year-class was produced in the Pacific in 2010 (Furuichi et al., 2022). Furthermore, sardine schools were hardly observed in the coastal areas of the SJ-ECS in spring 2014 and 2019. Sardine catches in the areas by Japanese vessels abruptly decreased to 10–30% in 2014 and 2019 compared to the prior years (Fig. 1c), as did catches by South Korean vessels (FAO, 2021), suggesting that sardines were sparse in the SJ-ECS (Fig. 1a). Numbers of eggs and larvae in spawning surveys and catches of age-0 juveniles in Japanese coastal areas during summer to autumn were also low in these years (Fig. 1c, Supplementary Fig. S1). Fortunately, sardine schools returned to Japanese coasts in spring in the following years (2015 and 2020). Nevertheless, despite the likely limited reproduction in 2014 and 2019 in the SJ-ECS, age-1 fish hatched in 2014 and 2019 were present in the 2015 and 2020 catches in proportions comparable to other common years (Fig. 1c). These observations raise the question of the origin of the recruits: are eggs, larvae and juveniles in the SJ-ECS the only source of recruits for the Tsushima Warm Current subpopulation?

The origin and nursery grounds of fish can be inferred from isotopic signatures in otoliths, the calcium carbonate formed in the inner ear (e.g. Rooker et al., 2008). The stable oxygen isotope value ($\delta^{18}O$) of fish otoliths is influenced negatively by temperature (for Japanese sardine, Sakamoto et al., 2017) and positively by seawater $\delta^{18}O$, and seawater $\delta^{18}O$ is strongly correlated with salinity (LeGrande & Schmidt, 2006). The stable carbon isotope ($\delta^{13}C$) of the otolith reflects the metabolic rate and the $\delta^{13}C$ of prey and dissolved inorganic carbon (Chung et al., 2019). These values may therefore differ among fish from different regions, allowing discrimination of nursery areas (Rooker et al., 2008; Sakamoto et al., 2020) and migration routes (Darnaude & Hunter, 2018; Sakamoto et al., 2019). Recently, Aono et al. (2024) found that otolith $\delta^{18}O$ profiles of age-0 sardines captured in the SJ-ECS in late summer consistently show marked decreasing trends, reflecting the significant seasonal warming of the region (Supplementary Fig. S2). Significant deviations from such trends may thus indicate different distributions in the first year of life.

We aimed to identify the recruitment sources of sardine in the SJ-ECS. To this end, otolith isotope ratios were analysed from age-0 and age-1 of 2010 and 2013–2015 year-classes of sardine caught in the SJ-ECS and western North Pacific during summer to autumn and the following spring, respectively (Fig. 1a). The periods include the key 2010 and 2014

year-classes of which age-1 fish were abundant despite the low catch of age-0 in the SJ-ECS (Fig. 1c). If juveniles that grew near the Japanese coast in the SJ-ECS are the main source of recruitment, as conventionally assumed, the otolith signatures of age-0 and age-1 fish should be similar, but this was not the case.

Materials and Methods

Otolith sample collection

To represent the entire nursery grounds of sardine in the SJ-ECS, otolith samples were collected from sardines captured in 2010–2011 and 2013–2016 in three major fishing areas, namely the regions around West Kyushu, the Oki Islands and the Noto Peninsula (Fig. 1a). The fish were captured in purse or set net fisheries or in midwater trawls during cruise surveys. Fish < 15 cm standard length (SL) captured during July to December were considered age-0 fish, and those < 16 cm SL captured during January to June were age-1 fish. To represent age-0 and 1 fish of the 2010 and 2013–2015 year-classes in each region, 2–8 individuals per sampling batch were selected from 1–3 sampling batches, except for age-0 of the 2010 and 2014 year-classes around the Noto Peninsula, as catch there was very low (Table 1). The 2015 year-class around the Oki Islands was sampled more frequently from September 2015 to May 2016 to observe seasonal variations in the proportions of different recruitment sources.

Table1. Metadata of collected samples from each region (*includes high-resolution data from Aono et al., 2024, **all data from Sakamoto et al., 2022).

Region	Year-class	Age	Collection Dates	SL (mm)	N spring	N summer
West Kyushu	2010	0	30 Aug, 31 Aug 2010	125.4±6.5	10	10
	2013	0	13 Sep, 4 Oct 2013	139.8±5.6	12	12
	2014	0	25 Aug, 2014	132.8±7.3	6	6
	2015	0	2 Sep, 12 Sep 2015	118.8±5.5	6*	6*
	2010	1	11 Jan, 2011	147.8±1.9	6	6
	2013	1	19 Jan, 25 Feb, 13 Mar 2014	149.1±2.6	19	12
	2014	1	29 Jan, 13 Feb, 17 Mar 2015	152.2±2.3	17	5
	2015	1	17 Jan, 2016	138.2±5.9	12	3
Oki Islands	2010	0	14 Jul, 2010	97.9±4.0	6	6
	2013	0	3 Sep, 22 Nov, 12 Dec 2013	134.1±8.5	22	19
	2014	0	26 Aug, 8 Oct 2014	124.2±9.7	15	11
	2015	0	1 Sep, 5 Nov, 1 Dec 2015	127±13.0	21	10
	2010	1	22 Apr, 13 May 2011	135.9±10.2	14	14
	2013	1	7 Apr, 20 May 2014	149.2±6.0	16	8
	2014	1	24 Feb, 25 Feb 2015	143.9±6.2	17	6
	2015	1	18 Feb, 8, 9,14 Mar, 12 Apr, 19, 20, 24, 30 May 2016	146.5±5.0	35	33
Noto Peninsula	2010	0	-	-	0	0
	2013	0	11 Jul, 2 Sep, 12 Sep 2013	85.8±13.5	25	12
	2014	0	-	-	0	0
	2015	0	23 Aug, 27 Aug, 8 Sep 2015	93.2±15.3	20*	13*
	2010	1	17 Mar, 11 May 2011	132.5±3.9	16	16
	2013	1	21 Apr, 25 Apr, 29 May 2014	140.9±3.8	22	11
	2014	1	16 Apr, 23 Apr, 8 May 2015	142.3±4.9	30	15
	2015	1	10 Mar, 11 Apr 2016	144.4±12	11	4
Pacific Offshore	2010	0	28 Sep, 1, 2, 4, 7 Oct 2010	115.5±5.7	25**	25**
	2013	0	-	-	0	0
	2014	0	23 Sep, 24 Sep 2014	130.1±4.1	29**	29**
	2015	0	18 Sep, 19 Sep, 20 Sep, 21 Sep 2015	131.1±5.7	30**	30**
				(Total)	442	322

Otolith processing, microstructure and isotope analyses

Microstructure analysis was performed on the otoliths to record the position and width of the daily increments during early life stages. For both age-0 and age-1 samples, the otolith portions formed during 0–60 days post hatch (dph), representing the spring season, and 106–120 dph for more than half of the samples, representing summer, were extracted as powder using a high-precision micro-milling system Geomill 326 (Izumo-web, Japan). The $\delta^{18}O$ and $\delta^{13}C$ of these powders were measured with isotope ratio mass spectrometers with an analytical precision better than ± 0.13 and 0.11‰, respectively, based on the methods described by Shirai et al. (2018) and Ishimura et al. (2004). Previously published

data from age-0 sardines collected in the Pacific offshore region in 2010, 2014 and 2015 (Sakamoto et al., 2022) and in the SJ-ECS in 2015 (Aono et al., 2024) were also included in the following analyses to allow more comprehensive comparisons (Table 1). See Supplementary Materials and Methods for more details.

Definitions of the "locals", "nonlocals" and "Pacific-offshores"

The otolith δ^{18}O of the age-0 sardine in the SJ-ECS and age-1 around West Kyushu generally showed a marked decline from spring to summer and lower values in summer (See Results, Fig. 2a). However, some age-1 fish caught from around the Oki Islands and the Noto Peninsula showed higher summer otolith δ^{18}O than those observed in the age-0 fish (Fig. 2b), indicative of a different nursery area. Thus, individuals captured in the SJ-ECS can be split into two groups, the "locals" which likely grew up in the SJ-ECS and the "nonlocals" which potentially did not, based on the otolith δ^{18}O for summer. For each year-class, the highest otolith δ^{18}O value of the age-0 sardine in the SJ-ECS and age-1 around the West Kyushu were defined as the threshold, and the individuals with lower or equal summer otolith δ^{18}O than the threshold were designated as "locals" and those with higher as "nonlocals". The age-0 in the SJ-ECS without the measurement of summer otolith δ^{18}O was also assigned to the "locals" as they likely grew up in the SJ-ECS. Age-1 around the Oki Islands and the Noto Peninsula lacking otolith δ^{18}O for summer were later categorized as either "locals" or "nonlocals" using a linear discriminant analysis based on the values for spring (see below). Age-0 sardines collected in the subarctic offshore region in the North Pacific were defined as "Pacific-offshores".

Discrimination of locals and nonlocals

To understand the differences in early life-history traits among locals, nonlocals and Pacific-offshores, differences in otolith δ^{18}O and δ^{13}C for spring and otolith radius at 60 dph were tested using a multivariate analysis of variance (MANOVA). Data of locals and nonlocals of all 4 year-classes were pooled for MANOVA. Data from lower outliers in δ^{18}O of locals detected by the boxplot method (< –1.56 ‰), likely from individuals raised in coastal and low-salinity waters, were removed to avoid violation of normality. Tests for multivariate normality, multicollinearity, linearity, homogeneity of covariances and variance were performed before MANOVA (see Supplementary Materials and Methods for details and their results). The non-parametric Kruskal–Wallis test and Games–Howell test were used for post-hoc tests and pairwise comparisons.

Given the significant differences in otolith δ^{18}O and δ^{13}C for spring and otolith radius at

60 dph, and the roughly linear relationships between the variables, a linear discriminant function analysis was performed to classify age-1 fish whose otolith δ^{18}O in summer was not analysed. A linear discriminant function was developed using the three variables of locals and nonlocals of all year-classes as learning data, and applied to unknown age-1 data to predict the most likely classification. The accuracies of the prediction models were estimated by leave-one-out cross-validation. These analyses were performed using Python 3.8.8 with Scikit-learn 0.24.1 library (Pedregosa et al., 2011).

Prediction of potential nursery areas of the nonlocals

To understand the origin of nonlocals, possible distributions during their first spring and summer were inferred from comparison between the predicted isoscape and observed otolith δ^{18}O (Supplementary Methods). As the distributions may be either within the SJ-ECS or in the western North Pacific, we made inferences for both possibilities. Briefly, the isoscapes of otolith δ^{18}O for spring and summer were estimated based on mean temperature and salinity distributions at 10 m depth during 0–60 and 106–120 days from the assumed hatch dates (mid-April to mid-May, Supplementary Fig. S1) and empirical relationships between otolith δ^{18}O and temperature and δ^{18}O of seawater and seawater δ^{18}O and salinity. The temperature and salinity distributions were obtained from data-assimilated hydrodynamic models for each region. The model grid points whose predicted otolith δ^{18}O was within the range of the mean ± 1 standard deviation (SD) of the otolith δ^{18}O of nonlocals of each year-class were considered as potential distributions. See Supplementary Materials and Methods and Supplementary Fig. S3 for further details and accuracy assessments of the hydrodynamic models.

Results

Seasonal profiles of otolith $\delta^{18}O$

Otolith δ^{18}O of the age-0 fish captured in the SJ-ECS (around West Kyushu, the Oki Islands and the Noto Peninsula) during 2010 and 2013–2015 seasonally decreased from –0.7 ± 0.4 ‰ (mean ± 1 SD) in spring (0–60 dph) to –1.5 ± 0.4 ‰ in summer (106–120 dph) (the locals, Fig. 2a). However, while some of the age-1 fish in the SJ-ECS showed similarly low δ^{18}O for summer (the locals), a number of age-1 fish in the SJ-ECS did not (the nonlocals, Fig. 2b). Otolith δ^{18}O of age-0 from the offshore subarctic North Pacific (the Pacific-offshores) showed slight seasonal increases (spring: –0.1 ± 0.3 ‰, summer: 0.1 ± 0.3 ‰, Fig. 2c). The summer otolith δ^{18}O values were significantly lower in age-0 fish in SJ-ECS than in Pacific-offshores, and the values of age- 1 fish in SJ-ECS were distributed among both groups (Fig. 2d). For each year-class and sampling region

analysed, almost all age-1 fish from West Kyushu showed a seasonal decrease in otolith $\delta^{18}O$ (spring: –0.6 ± 0.3 ‰, summer: –1.7 ± 0.4 ‰, also categorized as locals, Fig. 3), and some age-1 fish from the Oki Islands and Noto Peninsula showed non-decreasing trends (the nonlocals, spring: –0.3 ± 0.2 ‰, summer: –0.2 ± 0.3 ‰, Fig. 3). Exceptionally low $\delta^{18}O$ values in spring between –2.5 and –1.6 ‰ were observed in some age-0 and age-1 captured in 2014, which were consistent with the reported values of larvae captured in the less-saline bay near Noto Peninsula (–2.4 to –1.0‰, Nishida et al., 2020).

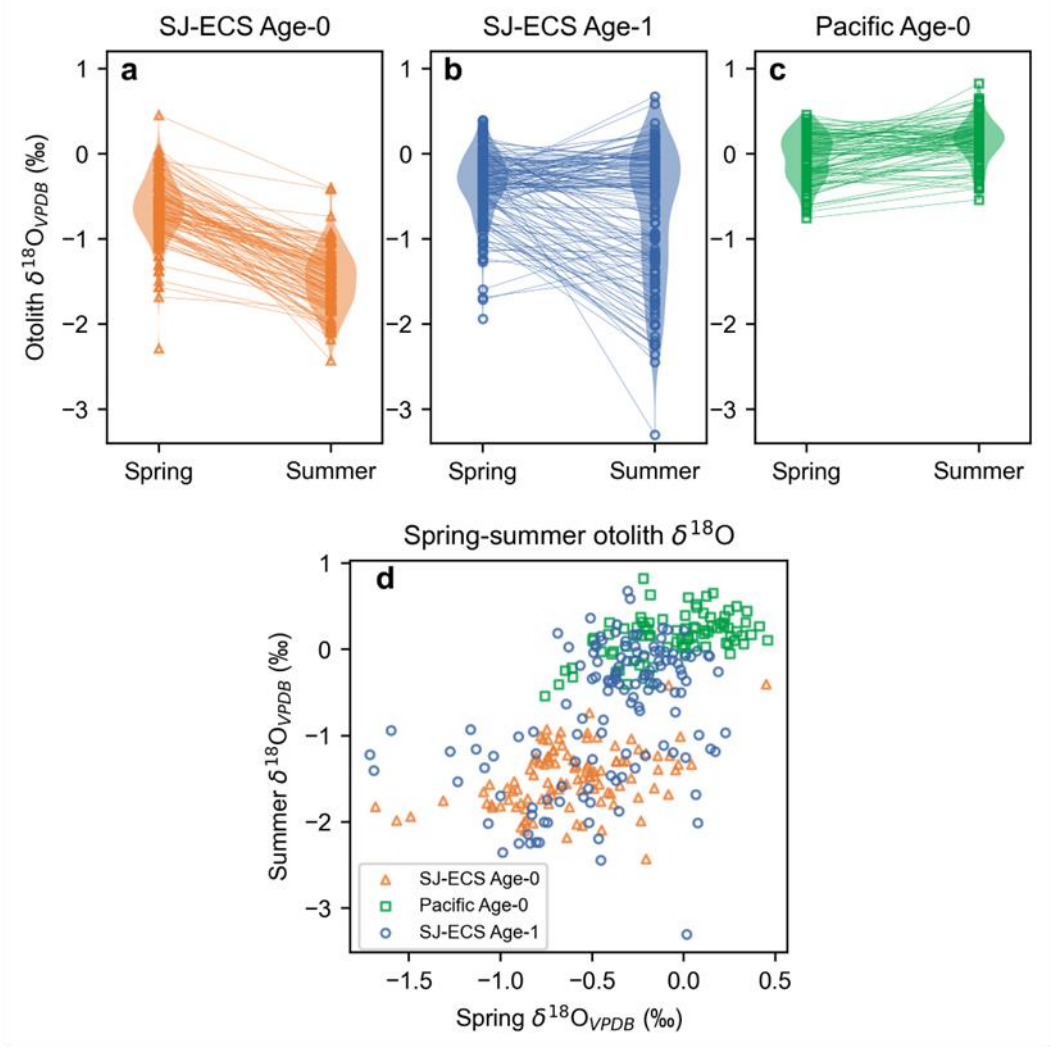

Figure 2. Otolith $\delta^{18}O$ profiles (spring: 0-60 dph, summer: 106-120 dph) of age-0 (a) and age-1 (b) sardines captured in the Sea of Japan and East China Sea, and age-0 fish from the subarctic offshore area in the Pacific (c). Data for all year-classes analysed are pooled and plotted with violin plot representing data density. Spring and summer otolith $\delta^{18}O$ values for each individual are also shown as a scatter plot (d).

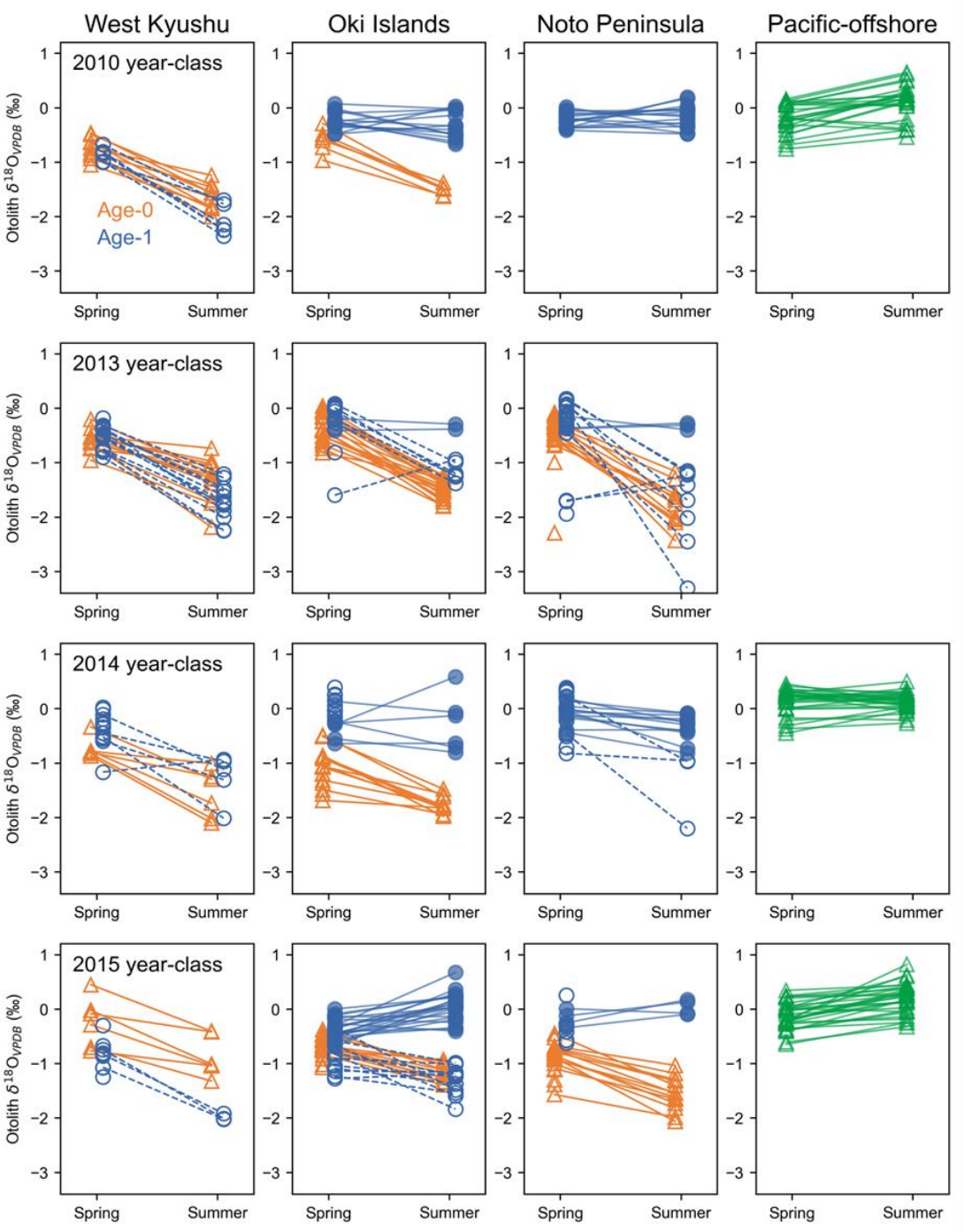

Figure 3. Year-class variations of seasonal profiles of otolith $\delta^{18}O$ in age-0 (orange) and age-1 (blue) sardines captured around West Kyushu (first column), the Oki Islands (second column), Noto Peninsula (third column) and Pacific offshore (fourth column). Data of 2010 2013, 2014 and 2015 year-classes are presented in each row from the top. Data of age-1 (blue) defined as the locals is shown in open circles and dotted lines and that of nonlocals is shown in filled circles with solid lines. Data of age-0 is shown in triangles with solid lines.

283
284

285 *Otolith δ^{18}O and δ^{13}C and otolith radius in spring*

286 Spring otolith δ^{18}O and δ^{13}C values and otolith radius at 60 dph of the locals, nonlocals
287 and Pacific-offshores were significantly different between groups (Fig. 4a, b, MANOVA,
288 $F(6, 724) = 57.943$, $p < 2.2*10^{-16}$). Post-hoc Kruskal–Wallis test showed that δ^{18}O and
289 otolith radius had significant differences among groups (δ^{18}O: Chi square = 139.0, p =
290 $6.2*10^{-31}$, df = 2, δ^{13}C: Chi square = 3.57, p = 0.17, df = 2, otolith radius: Chi square =
291 36.0, p =$1.5*10^{-8}$, df = 2). Pairwise comparisons using the Games–Howell test showed
292 that nonlocals had significantly higher mean otolith δ^{18}O and otolith radius at 60 dph than
293 locals (adjusted p value < $2.0*10^{-16}$ and = $1.7*10^{-10}$, respectively, Supplementary Table
294 S1), and lower mean otolith δ^{18}O than the Pacific-offshores (adjusted p value = $7.6*10^{-6}$).
295 Despite the significant difference in the mean otolith δ^{18}O, the overall value ranges of the
296 nonlocals consistently included those of the Pacific-offshores (Fig. 4a, b) in each year-
297 class (Fig. 4c-j). Higher otolith δ^{18}O that appeared in the Pacific-offshores (> 0.2‰) was
298 hardly observed in the nonlocals, which primarily came from individuals that hatched
299 earlier (Fig. S4). Cross-validation of the linear discriminant function analysis of locals
300 and nonlocals of all year-classes using the three variables correctly classified a total of
301 263 of 288 individuals (92%). Out of 218 individuals classified as locals, 205 (96%) were
302 actually locals and out of 70 individuals classified as nonlocals, 58 (83%) were actually
303 nonlocals. Based on the discriminant function, the 45 unclassified age-1 fish were divided
304 into 22 locals and 23 nonlocals.

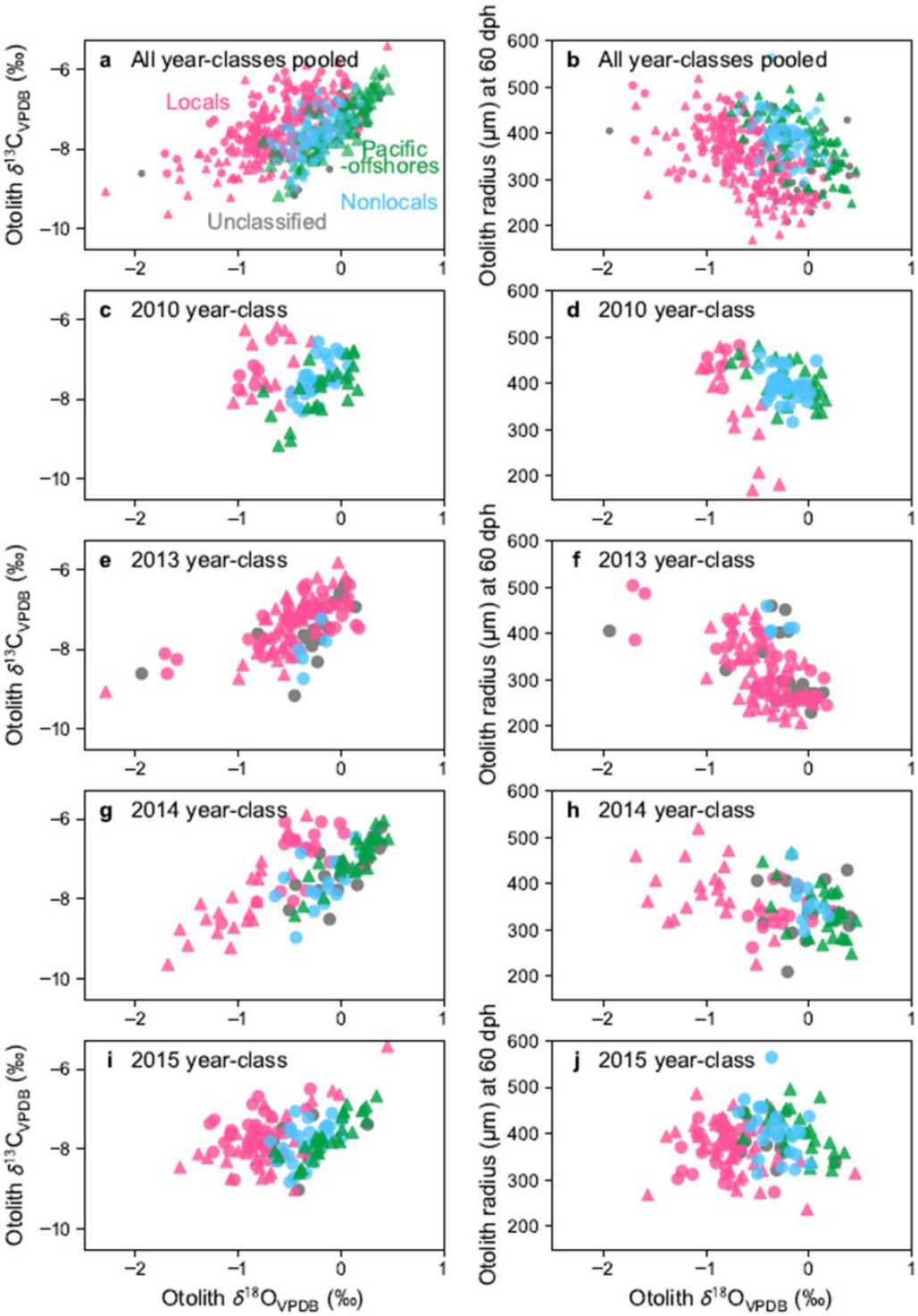

Figure 4. Relationships between otolith $\delta^{18}O$ and $\delta^{13}C$ for spring (a, c, e, g, i) and between otolith $\delta^{18}O$ for spring and otolith radius at 60 dph (b, d, f, h, j) for all year-classes pooled (a, b), 2010 year-class (c, d), 2013 year-class (e, f), 2014 year-class (g, h) and 2015 year-class (l, j). The locals are shown in pink, the nonlocals in light blue and the pacific-offshores in green. Gray plots are age-1 fish that are unclassified due to the lack summer otolith $\delta^{18}O$. Circles and triangles show age-1 and age-0 fish, respectively.

305

306

307 *Seasonal and inter-annual variation in locals/nonlocals proportions in the Sea of Japan*

308 To understand the timing of arrival of the nonlocals, 2015 year-class around the Oki
309 Islands was repeatedly sampled from September 2015 to May 2016. From September to
310 December 2015, all 21 fish in the 2015 year-class were locals by definition, and all 10
311 otolith $\delta^{18}O$ values analysed for the summer were lower than –0.9 ‰ (Fig. 5a). The
312 proportion of the nonlocals increased towards spring in 2016: one in 5 (20%) in February,
313 4 in 12 (33%) in March, 5 in 5 (100%) in April and 13 in 13 (100%) in May were nonlocals
314 (Fig. 5a). The proportions of locals and nonlocals in April and May, the main spawning
315 season in the Sea of Japan, showed consistent inter-annual fluctuations around the Oki
316 Islands and Noto Peninsula (Fig. 5b). Note that because no age-1 samples were available
317 from the Oki Islands in April and May 2015, the samples caught around the Oki Islands
318 in February 2015 were used for comparison instead. As the locals/nonlocals proportions
319 in individuals predicted by linear discriminant analysis were similar for individuals
320 grouped based on summer otolith $\delta^{18}O$, we considered the predictions to be largely
321 accurate. In 2011, 2015 and 2016, the nonlocals were the majority, with a proportion of
322 80–100% around both the Oki Islands and the Noto Peninsula (Fig. 5b). Additionally, the
323 8 age-1 individuals captured in March 2011 around Noto Peninsula were all nonlocals
324 (Fig. 3, not shown in Fig. 5). Only in 2014, when total sardine catch in SJ-ECS decreased
325 significantly, locals constituted the majority around both the Oki Islands and the Noto
326 Peninsula, at 75% and 73% respectively.

327

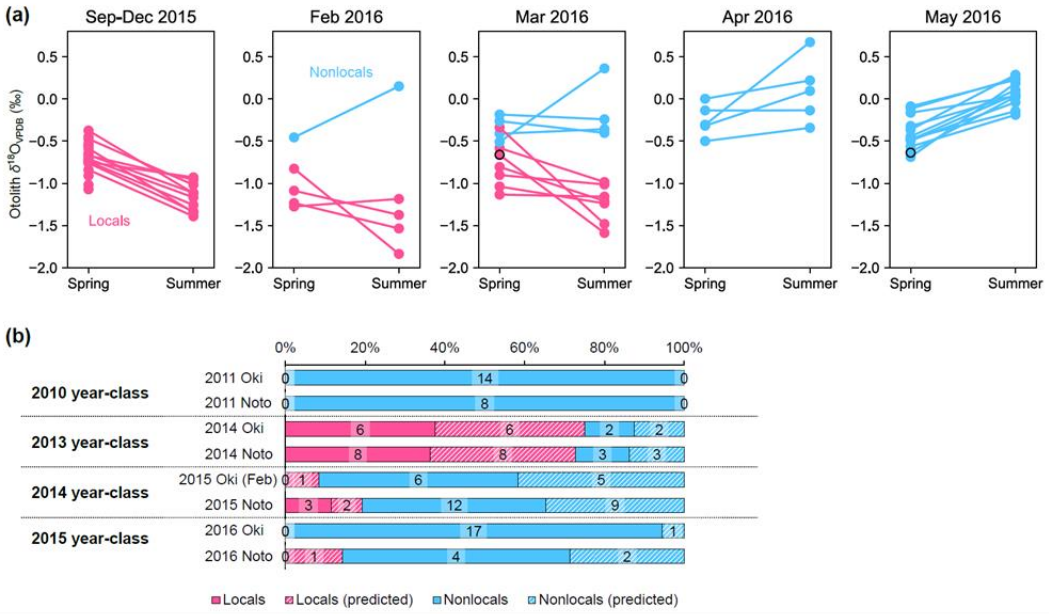

Figure 5. Otolith $\delta^{18}O$ profiles of 2015 year-class repeatedly sampled from September 2015 to May 2016 around the Oki Islands (a). Data of individuals classified by discriminant analysis is shown in black edge plots. Inter-annual variation of locals/nonlocals proportions in age-1 fish captured during spring (April to May, except for those around the Oki Islands 2015) (b). The numbers show the number of individuals in each group. Filled and meshed bars represent individuals that have and lack otolith $\delta^{18}O$ measurement for summer, respectively.

Potential nursery areas of nonlocals in spring and summer

The distribution of the nonlocals in 2015 year-class during spring (0–60 dph, of which median date corresponding to mid-May to mid-June assuming hatch dates as mid-April to mid-May) was predicted to be either the southern coastal areas in the Sea of Japan (Fig. 6a) or the offshore area along the Kuroshio Extension in the North Pacific (Fig. 6b). For summer (106–120 dph, corresponding to late July to late August), the predicted distributions shifted northward to the northern coastal areas of the Sea of Japan (Fig. 6a) or the subarctic Oyashio region north of 42°N (Fig. 6b). The predicted patterns were similar for the nonlocals of the 2013 and 2014 year-classes (Supplementary Fig. S5).

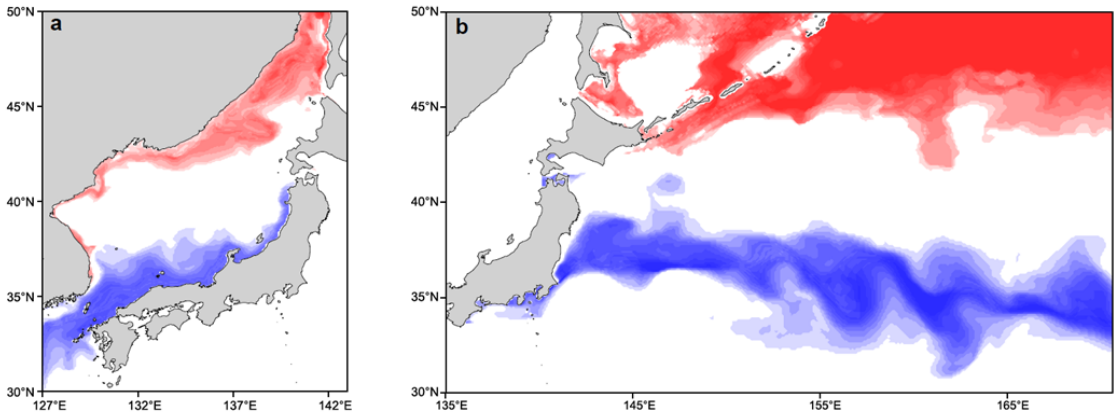

Figure 6. Potential distribution of migrants of 2015 year-class during first spring (0-60 dph, blue) and summer (106-120 dph, red) in the Sea of Japan (a) and the North Pacific (b) predicted based on otolith $\delta^{18}O$ and hydrodynamic models. Each light color shade shows the prediction for each assumed hatch date that were moved in 3 days intervals between mid-April and mid-May. The areas with deep colors are where such shades overlapped. See supplementary information for 2013 and 2014 year-class.

Discussion

We examined the stable isotope ratios of the otoliths of age-0 and age-1 Japanese sardine captured in the region in 2010–2011 and 2013–2016 to test the conventional hypothesis of self-recruitment of the subpopulation in the SJ-ECS. Most age-0 fish in the SJ-ECS and age-1 fish from West Kyushu showed a significant seasonal decrease in otolith $\delta^{18}O$ (Fig. 2a), reflecting the negative correlation between otolith $\delta^{18}O$ and temperature (Sakamoto et al., 2017) and the significant seasonal warming in the SJ-ECS (Supplementary Fig. S2). In contrast, a number of age-1 fish collected in the Sea of Japan had higher otolith $\delta^{18}O$ values for summer and mostly lacked such significant decreases in otolith $\delta^{18}O$ (Fig. 2b, d), strongly suggesting that they were distributed in a different region. We therefore conclude that juveniles that grew up in the Japanese coastal areas of the SJ-ECS (i.e., locals) are not the only source of recruitment to the SJ-ECS subpopulation, and that there are significant contributions from those that have migrated from other regions (i.e., nonlocals).

Nonlocals, who have a different migration pattern from the locals, are probably more important as a source of recruitment. The differences in otolith isotopes and radius at 60 dph indicate that the nursery areas of locals and nonlocals are not common from the early life stage (Fig. 4a, b). Analysis of the repeatedly sampled 2015 year-class around the Oki Islands showed that the locals dominate in autumn (September to December), but the

nonlocals increase from winter (February) onwards and completely replace the locals in spring (April and May) (Fig. 5a). Together with the fact that the nonlocals were found from the Sea of Japan but not from the West Kyushu in the East China Sea (Fig. 3), nonlocals were likely distributed somewhere north of the coastal areas during summer to autumn and migrated south during winter in the Sea of Japan. In spring, the peak season when schools of spawning adult fish arrive on the coast of the Sea of Japan, the nonlocals generally dominated age-1 fish in the Sea of Japan, the only exception being in 2014, when the numbers of age-1 fish and spawning fish were exceptionally low (Fig. 5b). This suggests that it is the nonlocals that move around the Sea of Japan in winter to spring along with the schools of spawning adult fish and therefore mainly recruit there. In addition, the abrupt decrease in catch in 2014 is likely a consequence of the change in the migration pattern of the nonlocals and accompanying adults.

The key question is where the nonlocals came from. Predictions of distribution provided two hypotheses for movement patterns during the first spring and summer (Fig. 6a, b), namely from the southern coastal areas of the SJ-ECS to the northern coastal areas of the Sea of Japan, and from the Kuroshio Extension area to the subarctic Oyashio area in the western North Pacific. The first pattern is consistent with the hypothesis that eggs and larvae in the southwest Sea of Japan may have been transported to the offshore area by the offshore branch of the Tsushima Warm Current in 1970–80s (Muko et al., 2018). Sardines tend to expand their distribution with population growth (Barange et al., 2009), and adults were abundant in the northern Sea of Japan in summer in 1930–40s and 1970–80s when the biomass was high (Nakai, 1962; Dudarev & Kenya, 1988; Muko et al., 2018). Meanwhile, in the limited data from historical surveys and fisheries in the northern Sea of Japan, sardine eggs, larvae and age-0 fish were hardly caught even in 1930–40s and 1970–80s (Nakai, 1962; Dudarev & Kenya, 1988). In addition, if the nonlocals originated from the southern Sea of Japan or the East China Sea (Fig. 6a), the abundance or proportion of the age-1 nonlocals would likely decrease in spring 2015 due to the severely limited spawning off the Japanese coast in 2014 (Fig. 1b), but this was not the case (Fig. 5b).

We then consider the possibility that the nonlocals originated from the western North Pacific. The idea of sardine migration from the Pacific was originally put forward by Nakai (1962), who found that sardine catches per unit effort off the Korean peninsula were strongly correlated with catches off Hokkaido in the previous year (fished mainly on the Pacific side, see Fig. 1a) between 1929 and 1941. Baba (2021) also mentioned the

possibility of mixing based on the detection of infections of the parasite *Anisakis simplex*, which is prevalent in the western North Pacific and not in SJ-ECS, on adult sardines caught in SJ-ECS in February and March. Some pelagic species are already known to migrate into the Sea of Japan against the strong current towards the Pacific in the Tsugaru Strait (e.g., Japanese common squid *Todarodes pacificus* (e.g., Sakaguchi, 2010), Masu salmon *Oncorhynchus masou* (e.g., Sato & Shibuya, 2015)). In this study, otolith isotope ratios for spring and summer and microstructure signatures of the nonlocals differed from those of the locals, but were mostly within the value ranges seen for the Pacific-offshores (Figs. 2–4; Supplementary Fig. S4). In addition, the time series of recruitment and recruits per spawner estimated by current stock assessment models for the Pacific and Tsushima Warm Current stocks showed significantly similar fluctuations (Fig. S6; year-to-year differences in recruitment: Pearson's $r = 0.87$, $p = 6.7*10^{-15}$, in recruits per spawner: $r = 0.49$, $p = 5.7*10^{-4}$), indicating that the main recruitment sources of the two stocks are common. Why do the decadal variations in catches in the Pacific and the SJ-ECS synchronise, and why can age-1 fish be abundant in the SJ-ECS, as in 2011, 2015 and 2020, even though egg production and age-0 catches were severely limited in the previous year? These phenomena are clearly explained if the recruits in the SJ-ECS are mainly migrating from the Pacific.

Our results provide important implications for fisheries management and developments in stock assessment for Japanese sardine. The current stock assessment for the sardine subpopulations is subject to considerable uncertainty, as it is based on an incomplete understanding of recruitment processes. As the Tsushima Warm Current subpopulation may not be closed, the estimate of recruitment can be significantly biased depending on the recruitment of the Pacific subpopulation. Considerations for a move to models that address mixing by incorporating empirically estimated mixing rates (de Moor et al., 2017) or even removing management unit boundaries need to be started. Nevertheless, we cannot completely exclude the possibility that the nonlocals are a northward-migrating group within the Sea of Japan that has not yet been observed. Further efforts to confirm and quantify the potential migrants from the Pacific or possibly the northern Sea of Japan, ideally in international collaboration, are essential to improve fisheries management for this species. As the overlap in otolith chemical signatures can still indicate different origins in similar environments (Fig. 6a, b), extensive research using multidisciplinary approaches, including basic biological metrics (Neves et al., 2021), genomics (Teske et al., 2021), parasite load (Baba, 2021), environmental DNA (Jerde, 2021) and cruise surveys must be conducted.

Overall, the analyses of the otoliths revealed the complexity of the population structure of Japanese sardine. The abrupt declines in sardine catches in 2014 and 2019 not only motivated us to investigate population structure, but also helped us do so by naturally acting as a control experiment, thereby highlighting the importance of collecting samples and data during anomalous years. Decline in fisheries catches often raises questions about assumptions in management strategies and prompt studies on the migratory ecology of species (e.g., Rooker et al., 2008; Neat et al., 2014). Accumulated knowledge about population connectivity can lead to a change in management settings, ultimately leading to fish biomass recovery and sustainable fisheries under science-based management (Hilborn et al., 2020). A decline in catch, while not at all beneficial to fisheries in the short term, could lead to a healthier marine ecosystem with sustainable fisheries production if research communities respond correctly.

References

Alder, J., Campbell, B., Karpouzi, V., Kaschner, K., & Pauly, D. (2008). Forage fish: from ecosystems to markets. *Annual Review of Environment and Resources*, 33, 153-166.

Amemiya, I., Abe, T. (1933). On the geographic variation of sardine around Japanese coastal areas, especially in the Pacific side. *Suisan Gakkaihou*, 5 (4). (in Japanese)

Aono, T., Sakamoto, T., Ishimura, T., Takahashi, M., Yasuda, T., Kitajima, S., Nishida, K., Matsuura, T., Ikari, A., Ito, S. (2024). Estimation of migrate histories of the Japanese sardine in the Sea of Japan by combining the microscale stable isotope analysis of otoliths and a data assimilation model. arXiv:2402.18602 *(preprint).*

Baba, T. (2021). Molecular identification and prevalence of *Anisakis* larvae in Japanese sardine *Sardinops melanostictus* from Japanese waters. *Nippon Suisan Gakkaishi,* 87 (1), 52-54. (in Japanese)

Barange, M., Coetzee, J., Takasuka, A., Hill, K., Gutierrez, M., Oozeki, Y., van der Lingen, C., & Agostini, V. (2009). Habitat expansion and contraction in anchovy and sardine populations. *Progress in Oceanography,* 83, 251-260.

Cadrin, S. X., Goethel, D. R., Morse, M. R., Fay, G., & Kerr, L. A. (2019). "So, where do

469 you come from?" The impact of assumed spatial population structure on estimates of
470 recruitment. *Fisheries Research*, 217, 156-168.
471
472 Checkley Jr, D. M., Asch, R. G., & Rykaczewski, R. R. (2017). Climate, anchovy, and
473 sardine. *Annual Review of Marine Science*, 9, 469-493.
474
475 Chung, M., Trueman, C. N., Godiksen, J. A., Holmstrup, M. E., & Grønkjær, P. (2019).
476 Field metabolic rates of teleost fishes are recorded in otolith carbonate.
477 *Communications Biology,* 2, 1-10.
478
479 Cury, P.M., Boyd, I.L., Bonhommeau, S., Anker-Nilssen, T., Crawford, R.J., Furness,
480 R.W., Mills, J.A., Murphy, E.J., Österblom, H., Paleczny, M. & Piatt, J.F. (2011).
481 Global seabird response to forage fish depletion–one-third for the birds. *Science,* 334,
482 1703-1706.
483
484 Darnaude, A. M., & Hunter, E. (2018). Validation of otolith δ18O values as effective
485 natural tags for shelf-scale geolocation of migrating fish. *Marine Ecology Progress*
486 *Series,* 598, 167-185.
487
488 de Moor, C. L., Butterworth, D. S., & van der Lingen, C. D. (2017). The quantitative use
489 of parasite data in multistock modelling of South African sardine (Sardinops
490 sagax). *Canadian Journal of Fisheries and Aquatic Sciences,* 74, 1895-1903.
491
492 Donlon, C. J., Martin, M., Stark, J., Roberts-Jones, J., Fiedler, E., & Wimmer, W.
493 (2012). The operational sea surface temperature and sea ice analysis (OSTIA)
494 system. *Remote Sensing of Environment*, 116, 140-158.
495
496 Dudarev, V. S. & Kenya, V. S. (1988). Sardine in the North Pacific, *Living resources in*
497 *the Pacific*, (Fisheries Agency, *Nisso gyogyou kagaku gijutsu kyouryoku honyaku*
498 *insatsu bunken*), 72-81. (translated to Japanese)
499
500 FAO, Fishery and Aquaculture Statistics 2019, *FAO Yearbook*, (2021).
501
502 Furuichi, S., Yasuda, T., Kurota, H., Yoda, M., Suzuki, K., Takahashi, M., & Fukuwaka,
503 M. A. (2020). Disentangling the effects of climate and density-dependent factors on
504 spatiotemporal dynamics of Japanese sardine spawning. *Marine Ecology Progress*

505 *Series*, 633, 157-168.
506
507 Furuichi, S., Yukami, R., Kamimura, Y., Nishijima, S., & Watabe, R. (2022).
508 Subpopulation assessment and evaluation for the Pacific subpopulation of Japanese
509 sardine (fiscal year 2021). In *Marine fisheries subpopulation assessment and*
510 *evaluation for Japanese waters (fiscal year 2021/2022)*. (Fisheries Agency and
511 Fisheries Research and Education Agency of Japan, Yokohama, 2022) (in Japanese).
512
513 Hilborn, R., Amoroso, R.O., Anderson, C.M., Baum, J.K., Branch, T.A., Costello, C., de
514 Moor, C.L., Faraj, A., Hively, D., Jensen, O.P. & Kurota, H. (2020). Effective fisheries
515 management instrumental in improving fish subpopulation status. *Proceedings of the*
516 *National Academy of Sciences.* 117, 2218-2224.
517
518 Ishimura, T., Tsunogai, U., & Gamo, T. (2004). Stable carbon and oxygen isotopic
519 determination of sub-microgram quantities of $CaCO_3$ to analyze individual
520 foraminiferal shells. *Rapid Communications in Mass Spectrometry.* 18, 2883-2888.
521
522 Jerde, C. L. (2021). Can we manage fisheries with the inherent uncertainty from eDNA? *J.*
523 *Fish Biol.* 98, 341-353.
524
525 Kerr, L. A., Cadrin, S. X., & Kovach, A. I. (2014). Consequences of a mismatch between
526 biological and management units on our perception of Atlantic cod off New England.
527 *ICES Journal of Marine Science,* 71, 1366-1381.
528
529 LeGrande, A. N., & Schmidt, G. A. (2006). Global gridded data set of the oxygen isotopic
530 composition in seawater. *Geophysical Research Letters*, 33(12).
531
532 Morimoto, H. (2010) Temporal and spatial changes in the reproductive characteristics of
533 female Japanese sardine Sardinops melanostictus and their effects on the population
534 dynamics. *Bulletin of Japanese Society of Fisheries Oceanography*, 74, 35-45. (in
535 Japanese)
536
537 Muko, S., Ohshimo, S., Kurota, H., Yasuda, T., & Fukuwaka, M. A. (2018). Long-term
538 change in the distribution of Japanese sardine in the Sea of Japan during population
539 fluctuations. *Marine Ecology Progress Series,* 593, 141-154.
540

Muko, S., Takahashi M., Kurota, H., Yoda, M., & Hino, R. (2022). Subpopulation assessment and evaluation for the Tsushima Warm Current subpopulation of Japanese sardine (fiscal year 2021). In *Marine fisheries subpopulation assessment and evaluation for Japanese waters (fiscal year 2021/2022)*. (Fisheries Agency and Fisheries Research and Education Agency of Japan, Yokohama, 2022) (in Japanese).

Nakai, Z. (1962). Studies relevant to mechanisms underlying the fluctuation in the catch of the Japanese sardine, *Sardinops melanosticta. Japanese Journal of Ichthyology,* 9, 1-115.

Neat, F.C., Bendall, V., Berx, B., Wright, P.J., Ó Cuaig, M., Townhill, B., Schön, P.J., Lee, J. & Righton, D. (2014). Movement of Atlantic cod around the British Isles: implications for finer scale stock management. *Journal of Applied Ecology,* 51, 1564-1574.

Neves, J., Silva, A. A., Moreno, A., Verissimo, A., Santos, A. M., & Garrido, S. (2021). Population structure of the European sardine Sardina pilchardus from Atlantic and Mediterranean waters based on otolith shape analysis. *Fisheries Research,* 243, 106050.

Niino, Y., Furuichi, S., Kamimura, Y., & Yukami, R. (2021). Spatiotemporal spawning patterns and early growth of Japanese sardine in the western North Pacific during the recent subpopulation increase. *Fisheries Oceanography,* 30, 643-652.

Nishida, K., Yasu, A., Nanjo, N., Takahashi, M., Kitajima, S., & Ishimura, T. (2020). Microscale stable carbon and oxygen isotope measurement of individual otoliths of larvae and juveniles of Japanese anchovy and sardine. *Estuarine, Coastal and Shelf Science*, 245, 106946.

Okazaki, T., Kobayashi, T., & Uozumi, Y. (1996). Genetic relationships of pilchards (genus: Sardinops) with anti-tropical distributions. *Marine Biology*, 126, 585-590.

Oozeki, Y., Takasuka, A., Kubota, H., & Barange, M. (2007). Characterizing Spawning Habitats of Japanese Sardine, Sardinops Melanostictus, Japanese Anchovy, Engraulis Japonicus, and Pacific Round Herring, Etrumeus Teres, in the Northwestern Pacific. *California Cooperative Oceanic Fisheries Investigations Report,* 48, 191.

577 Pedregosa, F., Varoquaux, G., Gramfort, A., Michel, V., Thirion, B., Grisel, O., Blondel,
578 M., Prettenhofer, P., Weiss, R., Dubourg, V. & Vanderplas, J. (2011). Scikit-learn:
579 Machine learning in Python. *The Journal of Machine Learning Research,* 12, 2825-
580 2830.
581
582 Rooker, J. R., Secor, D. H., De Metrio, G., Schloesser, R., Block, B. A., & Neilson, J. D.
583 (2008). Natal homing and connectivity in Atlantic bluefin tuna populations. *Science,*
584 322, 742-744.
585
586 Sakaguchi, K. (2010). Migration of tagged Japanese common squid *Todarodes pacificus*,
587 in waters around Hokkaido. *Scientific Reports of Hokkaido Fisheries Experimental*
588 *Station,* 77, 45-72. (in Japanese)
589
590 Sakamoto, T., Komatsu, K., Shirai, K., Higuchi, T., Ishimura, T., Setou, T., Kamimura, Y.,
591 Watanabe, C. & Kawabata, A. (2019). Combining microvolume isotope analysis and
592 numerical simulation to reproduce fish migration history. *Methods in Ecology and*
593 *Evolution,* 10, 59-69.
594
595 Sakamoto, T., Komatsu, K., Yoneda, M., Ishimura, T., Higuchi, T., Shirai, K., Kamimura,
596 Y., Watanabe, C. & Kawabata, A. (2017). Temperature dependence of $\delta^{18}O$ in otolith
597 of juvenile Japanese sardine: Laboratory rearing experiment with micro-scale analysis.
598 *Fisheries Research,* 194, 55-59.
599
600 Sakamoto, T., Van Der Lingen, C. D., Shirai, K., Ishimura, T., Geja, Y., Peterson, J., &
601 Komatsu, K. (2020). Otolith $\delta^{18}O$ and microstructure analyses provide further evidence
602 of population structure in sardine *Sardinops sagax* around South Africa. *ICES Journal*
603 *of Marine Science,* 77, 2669-2680.
604
605 Sakamoto, T., Takahashi, M., Chung, M.T., Rykaczewski, R.R., Komatsu, K., Shirai, K.,
606 Ishimura, T. & Higuchi, T. (2022). Contrasting life-history responses to climate
607 variability in eastern and western North Pacific sardine populations. *Nature*
608 *Communications*, 13(1), 5298.
609
610 Sato, M., & Shibuya, K. (2015). Migration route, growth, and natal-river selectivity of
611 masu salmon *Oncorhynchus masou* released in the Yoneshiro River, *Aquaculture*
612 *Science,* 63(3), 283-290. (in Japanese)

Shirai, K., Koyama, F., Murakami-Sugihara, N., Nanjo, K., Higuchi, T., Kohno, H., Watanabe, Y., Okamoto, K. & Sano, M. (2018). Reconstruction of the salinity history associated with movements of mangrove fishes using otolith oxygen isotopic analysis. *Marine Ecology Progress Series*, 593, 127-139.

Tabachnick, B. G. & Fidell, L. S. (2012). *Using Multivariate Statistics*, 6th Edition, Pearson.

Teske, P.R., Emami-Khoyi, A., Golla, T.R., Sandoval-Castillo, J., Lamont, T., Chiazzari, B., McQuaid, C.D., Beheregaray, L.B. & van der Lingen, C.D. (2021). The sardine run in southeastern Africa is a mass migration into an ecological trap. *Science Advances*, 7, eabf4514.

Yasuda, T., Kitajima, S., Hayashi, A., Takahashi, M., & Fukuwaka, M. A. (2021). Cold offshore area provides a favorable feeding ground with lipid-rich foods for juvenile Japanese sardine. *Fisheries Oceanography,* 30, 455-470.

Supporting Information for:

Title

Fisheries shocks provide an opportunity to reveal multiple recruitment sources of sardine in the Sea of Japan

Contents:

Supplementary Material and Methods

Details in otolith processing, isotope analysis and length back-calculation

Collected fish were frozen after landing or on board at -20 °C, and thawed at a laboratory. After measurements of length and weight, the sagittal otoliths were extracted. The otoliths were cleaned using a thin brush and rinsed with fresh water. These otolith samples were processed in two different protocols, namely low-resolution analysis similar to Sakamoto et al. (2020) and high-resolution analysis similar to Aono et al. (2023). The majority of the otoliths were analysed using low-resolution protocol. In addition to these, high-resolution data from age-0 fish captured in 2015 around Kyushu and the Noto Peninsula (Aono et al., 2023) were also included in analyses to allow a more comprehensive comparison.

For low-resolution analysis, otoliths were embedded in Petropoxy 154 (Burnham Petrographics LLC) resin and kept at 80 °C for 12 h to cure. Otoliths were ground and polished until the core was revealed using sandpaper and alumina suspension (BAIKOWSKI International Corporation). Using an otolith measurement system (RATOC System Engineering Co. Ltd.), daily increments were examined along the axis in the post-rostrum from the core as far as possible. Daily increments could be identified until the edge for most otoliths of age-0 fish but not for those of age-1 fish, likely because the otolith growths became significantly slower during winter. The otolith portion formed during 0–60 dph, representing spring, was identified and milled out using a high-precision micro-milling system Geomill 326 (Izumo-web, Japan). For approximately half of the samples, the portion of the otolith formed during 106–120 dph was additionally milled out to represent values for summer. The milling depth for the spring and summer portions was 50 and 100 μm, respectively. The $\delta^{18}O$ and $\delta^{13}C$ of powdered samples were measured using an isotope ratio mass spectrometer (Delta V plus, Thermo Fisher Scientific) equipped with an automated carbonate reaction device (GasBench II, Thermo Fisher Scientific), and installed at the Atmosphere and Ocean Research Institute, the University of Tokyo, Chiba. Detailed analytical conditions have been reported elsewhere (e.g. Shirai et al. 2018), with minor modifications where 4.5-ml glass vials were used (Breitenbach & Bernasconi, 2011). All isotope values are reported using delta notation relative to the Pee Dee Belemnite. No correction was applied for the acid fractionation factor between calcite and aragonite [phosphoric acid–calcium carbonate reaction temperature 72 °C (Kim et al. 2007)]. Analytical precisions of $\delta^{18}O$ and $\delta^{13}C$ for international standards (NBS-19) were 0.06–0.13 (1σ) and 0.05–0.11 ‰, respectively. Because the difference between the acid fractionation factor of calcite and aragonite is temperature dependent

(Kim et al., 2007), 0.09 ‰ was subtracted from the $\delta^{18}O$ value to allow comparison with data analysed using another analysing system operating at 25 °C.

High-resolution analysis was performed for 17 otoliths of age-0 and age-1 fish captured in 2015. Otoliths were embedded in epoxy resin (p-resin, Nichika Inc.) and kept in a dryer at room temperature for more than a day to cure. Otoliths were grounded and polished until the core was revealed using sandpaper and alumina suspension (BAIKOWSKI International Corporation). Unfortunately, microstructure analysis was not performed for some of these otoliths. The otolith portions that were formed every 5–30 days or 30–160 μm were milled sequentially from the edge to the core using GEOMILL326. The $\delta^{18}O$ of collected otolith powders were determined by a customized continuous-flow isotope ratio mass spectrometry system (MICAL3c with IsoPrime100) at the National Institute of Technology, Ibaraki College, Hitachinaka, Japan (Ishimura et al., 2004; 2008; Nishida & Ishimura, 2017). Otolith powders were reacted with phosphoric acid at 25 °C, and the evolved CO_2 was purified and introduced into the mass spectrometry system. $\delta^{18}O$ values of each sample were reported in standard δ notation (‰) relative to the Vienna Pee Dee Belemnite (VPDB) standard. Analytical precisions were ± 0.1 ‰ for both $\delta^{18}O$ and $\delta^{13}C$. For otoliths for which microstructure analysis was not performed, the corresponding age range for each milling area was later estimated from distance from the core using the mean relationship between otolith radius and age of other fish captured in the same year, season and region. For comparison with the low-resolution data, the high-resolution data and data from Aono et al., (in revision) needed to be rescaled to spring (0–60 dph) and summer (106–120 dph) resolution. Therefore, $\delta^{18}O$ and $\delta^{13}C$ data for which the median of corresponding age range falls in 0–60 and 106–120 dph were averaged, linearly weighted by the width of the milling area.

Multivariate analysis of variance of otolith $\delta^{18}O$ and $\delta^{13}C$ for spring and SL_{60}

To test for the differences in otolith $\delta^{18}O$ and $\delta^{13}C$ for spring and otolith radius at 60 dph among locals, migrants and the Pacific-offshores, a multivariate analysis of variance (MANOVA) was performed, following Tabachnick et al. (2012). Data of locals and migrants of all 3 year-classes were pooled for MANOVA. Normality of each variable of each group was tested using Shapiro–Wilk's test, which showed significant violations of normality in $\delta^{18}O$ of locals ($p = 0.002$) and marginally in $\delta^{18}O$ of Pacific-offshores. Therefore, lower outliers in $\delta^{18}O$ detected in locals by the boxplot method (< -1.56 ‰), likely data of individuals that grew in coastal low-saline waters, were removed.

Multivariate normality was tested multivariate Shapiro–Wilk's test, which suggested significant violation ($p = 0.003$). Pearson's r between the variables was between -0.24 and 0.51, suggesting limited multicollinearity. No nonlinear relationship between variables in each group was evident in the scatter plots. As homogeneity of covariances was violated (Box's M-test, $p = 2.6*10^{-15}$), Pillai's multivariate statistic was used in MANOVA. Homogeneity of variance was tested by Levene's test, which suggested that the violation in $\delta^{13}C$ ($p = 0.005$), $\delta^{18}O$ ($p = 5.3*10^{-6}$) and otolith radius ($p = 6.9*10^{-5}$). Because some violations were thus detected in the assumption tests as above, $\alpha = 0.01$ was used as significance threshold in MANOVA to perform the test conservatively, and the non-parametric Kruskal–Wallis test and Games–Howell test were used in post-hoc tests and pairwise comparisons. These analyses were performed using R 4.1.0 with packages tidyverse 1.3,1, ggpubr 0.4.0, rstatix 0.7.0, car 3.0.11, broom 0.7.9 and GGally 2.1.2.

Prediction of potential nursery areas of the migrants

To understand the origin of migrants, potential distributions during their first spring and summer were inferred by comparing observed and predicted isoscape of otolith $\delta^{18}O$ using a hydrodynamic model (Aono et al., 2023). As the distributions can be either inside the SJ-ECS system or the western North Pacific, we made inferences for both patterns. To match the fish age to actual calendar dates, the hatch dates of migrants needed to be assumed. Spawning in the SJ-ECS system peaked during April to May in 2013–2015 (Supplementary Fig. S1). The most frequently occurred hatch dates of juveniles found in the Kuroshio-Oyashio transition zone were also between mid-April and mid-May during 2013–2015 (Niino et al., 2020). Based on these observations, the mean hatch date of the migrants was considered to be between 16th April and 16th May. For calculation of isoscapes, hatch date was assumed to be every three days between 16th April and 16th May. For each hatch date assumption, mean temperature and salinity distributions at 10m depth during 0–60 days (spring) and 106–120 days (summer) from hatch were calculated using daily reanalysis data provided by the data assimilated model JADE2 (Igeta et al., 2022) for the SJ-ECS system, and FRA-ROMS for the North Pacific (Kuroda et al., 2018). From these temperature and salinity distributions, the isoscape of otolith $\delta^{18}O$ was predicted following the relationships between otolith $\delta^{18}O$ and seawater temperature and $\delta^{18}O$, and between salinity and seawater $\delta^{18}O$ specifically developed for each region:

Otolith $\delta^{18}O$ = Seawater $\delta^{18}O$ – 0.18*Temperature (°C) + 2.69 (Sakamoto et al., 2017),

Seawater $\delta^{18}O = 0.23*Salinity – 7.54$ (for the SJ-ECS system, Aono et al., 2023)

Seawater $\delta^{18}O = 0.56*Salinity – 19.06$ (for the Pacific, Sakamoto et al., 2019).

The model grid points which predicted otolith $\delta^{18}O$ was within the range of the mean ± 1 standard deviation (SD) of the analysed otolith $\delta^{18}O$ of migrants of each year-class were considered as potential distributions. For visualization, the predicted distributions for each hatch date assumption were shown as translucent shades (alpha = 0.15) and overlaid in one figure using Matplotlib 3.3.4 in Python 3.8.8.

The accuracy of the hydrodynamic model directly affects the reliability of the predictions. JADE2 (Japan Sea Data Assimilation Experiment 2) is a data-assimilated hydrodynamic model aimed to realistically reproduce the current field of SJ-ECS system, maintained by Fisheries Research and Education Agency (Igeta et al., 2022). This model is based on DR_M (Hirose et al., 2013), and the sea surface height and temperature available from an AVISO product, and in situ observations conducted by Japanese prefectural institutes were assimilated into the model by an approximate Kalman filtering and nudging method. The model domain is meshed by 1/12° and 1/15° in the zonal and meridional directions, respectively. Because the accuracies of assessments of temperature and salinity for this model have not been published, we compared the modelled values to those observed by Argo floats (Supplementary Fig. S2). Argo float dataset Advanced automatic QC(AQC) Argo Data ver.1.2a distributed by JAMSTEC (Sato, 2014) was used for this comparison. The root-mean-square differences (RMSDs) between modelled and Argo float observed temperatures and salinities at depths shallower than 15m were 1.0–1.9 °C and 0.1–0.7, respectively, during February to September 2014 and 2015 (Supplementary Fig. S2). These differences corresponded to RMSD 0.2–0.3 ‰ in predicted otolith $\delta^{18}O$ (Supplementary Fig. S2). FRA-ROMS is an ocean forecast and reanalysis system based on the Regional Ocean Modelling System (ROMS) with three-dimensional variational analysis (Kuroda et al., 2016). The aim of this system is to realistically simulate mesoscale variations in the western North Pacific, and reproduce representative features of mesoscale variations such as the position of the Kuroshio path, variability of the Kuroshio Extension, and southward intrusions of the Oyashio (Kuroda et al., 2016). The RMSDs between sea surface temperature observed by satellite and reanalysed by FRA-ROMS, estimated at monthly intervals, were in the range 0.63–1.10 °C, corresponding to 0.11–0.20‰ in otolith $\delta^{18}O$ (Kuroda et al., 2016). The RMSDs between a monthly mean dataset of global oceanic salinity derived from Argo float observations and reanalysed salinity at

10 m depth were below 0.20 in the Kuroshio-Oyashio system, corresponding to 0.12‰ in seawater $\delta^{18}O$ (Sakamoto et al., 2019). These assessments show that the accuracies are comparable to the analytical precision of $\delta^{18}O$ of otolith and seawater, and variability of observed otolith $\delta^{18}O$ of the migrants.

Supplementary Figures

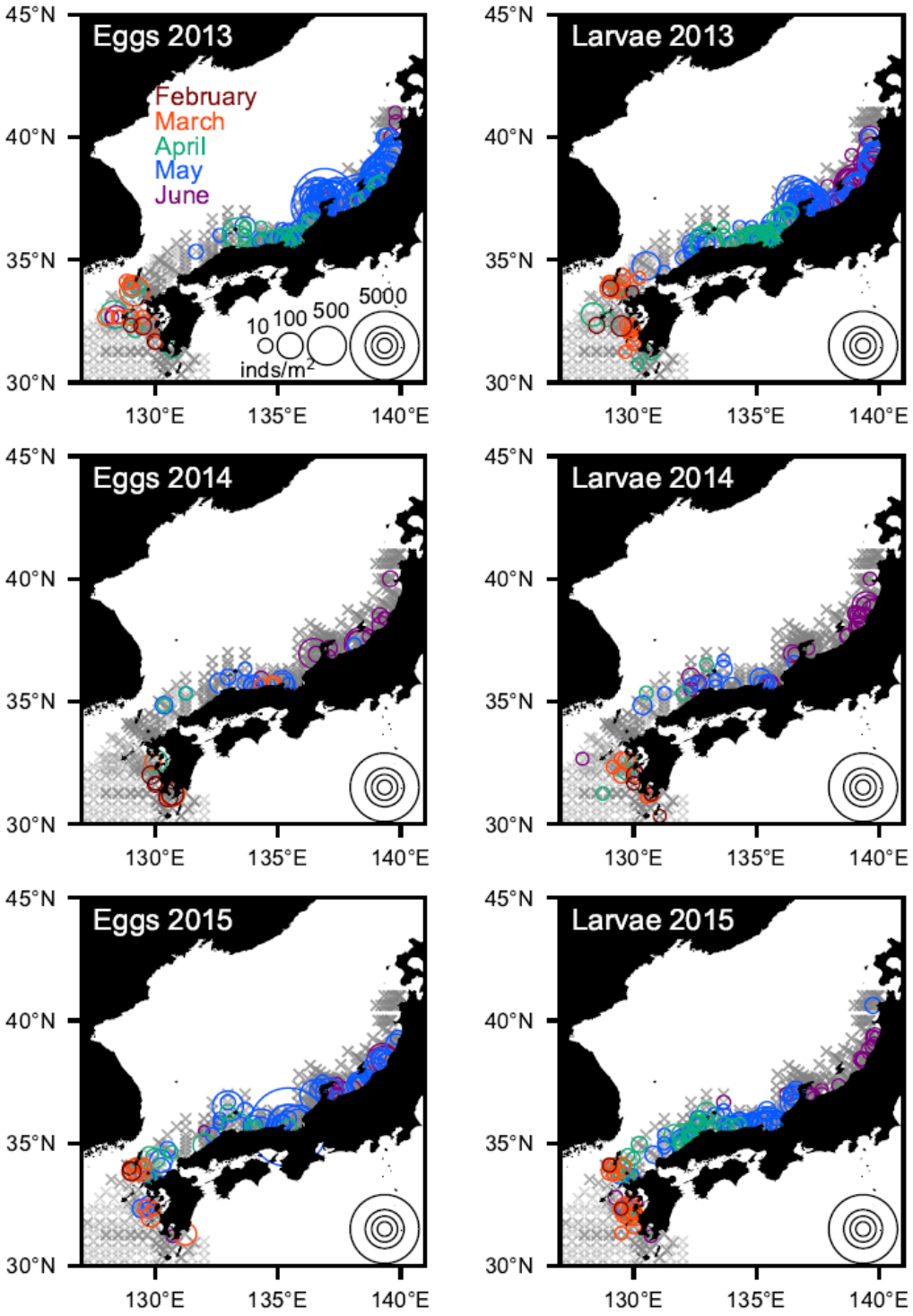

Supplementary Figure S1. Results of spawning surveys during February–June 2013–2015. The circles and crosses show the locations where eggs or larvae were and were not found, respectively. The sizes of the circle represent the density of eggs or larvae collected by NORPAC nets.

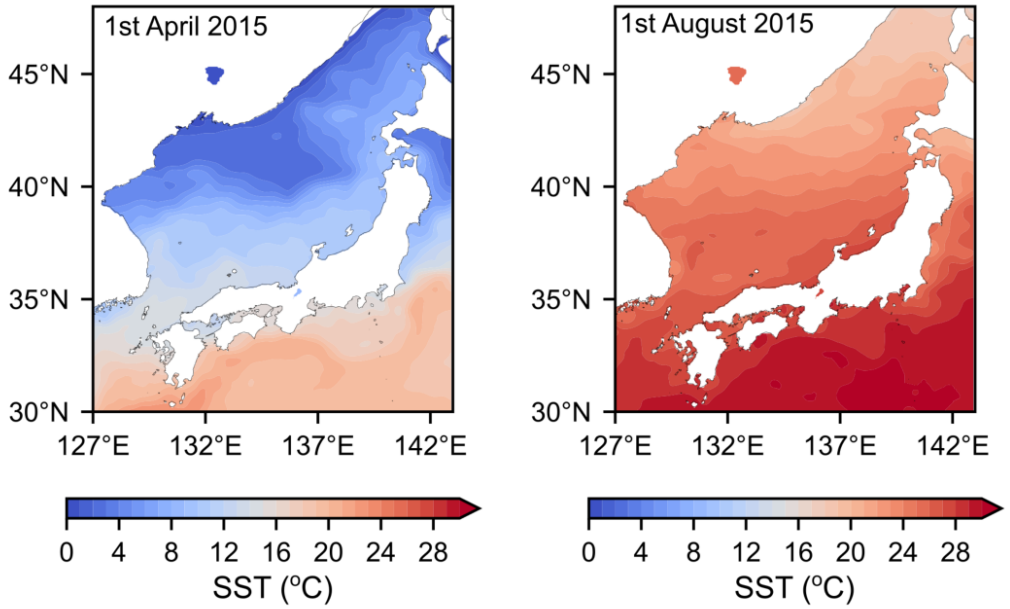

Supplementary Figure S4. Sea surface temperature on 1st April and 1st August 2015. Satellite-based product (the operational sea surface temperature and sea ice analysis (OSTIA) system, Donlon et al., 2012) was used.

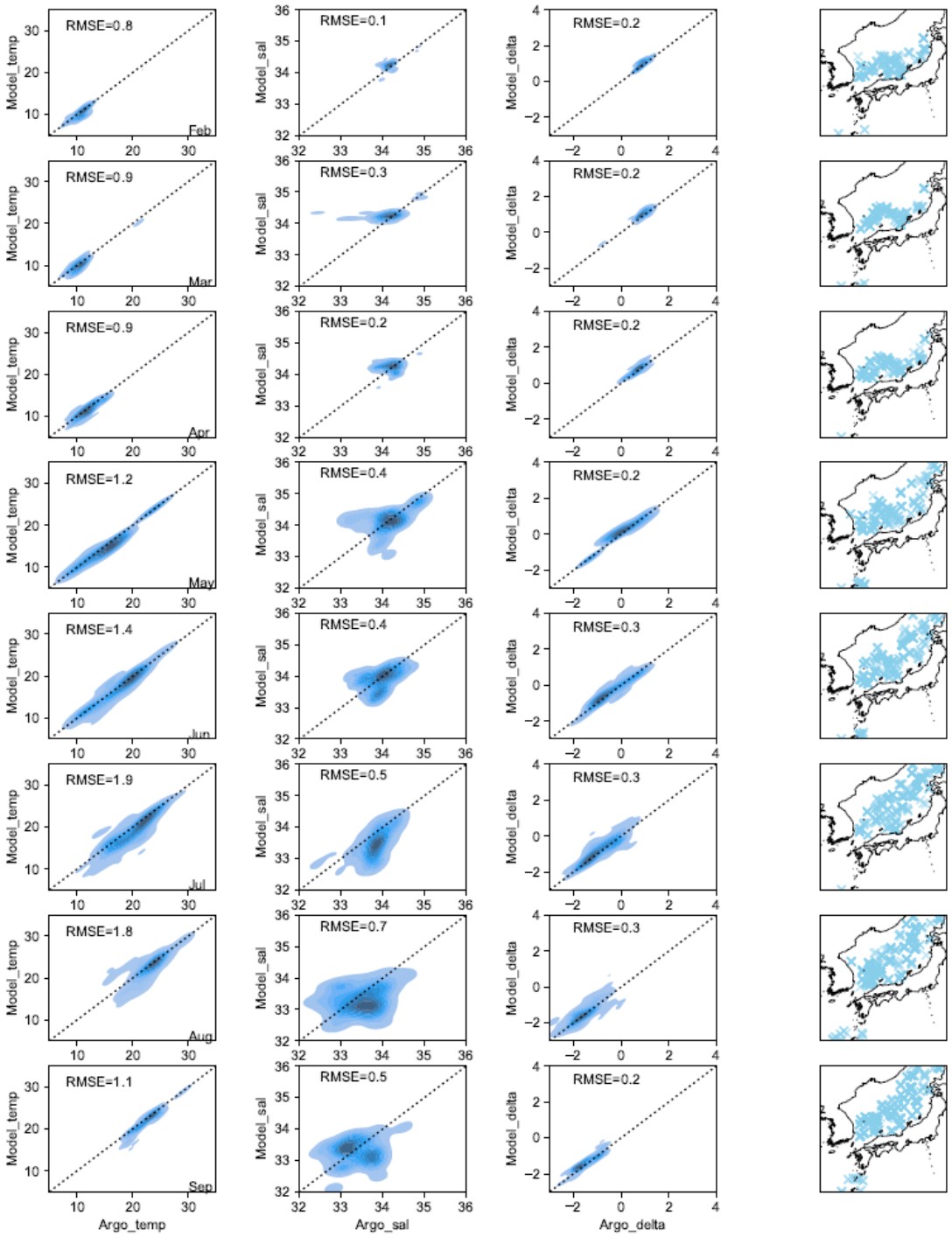

Supplementary Figure S3. Comparison of temperature (first column) and salinity (second column) modelled by JADE-2 model and those observed by Argo floats during February–September 2014–2015.

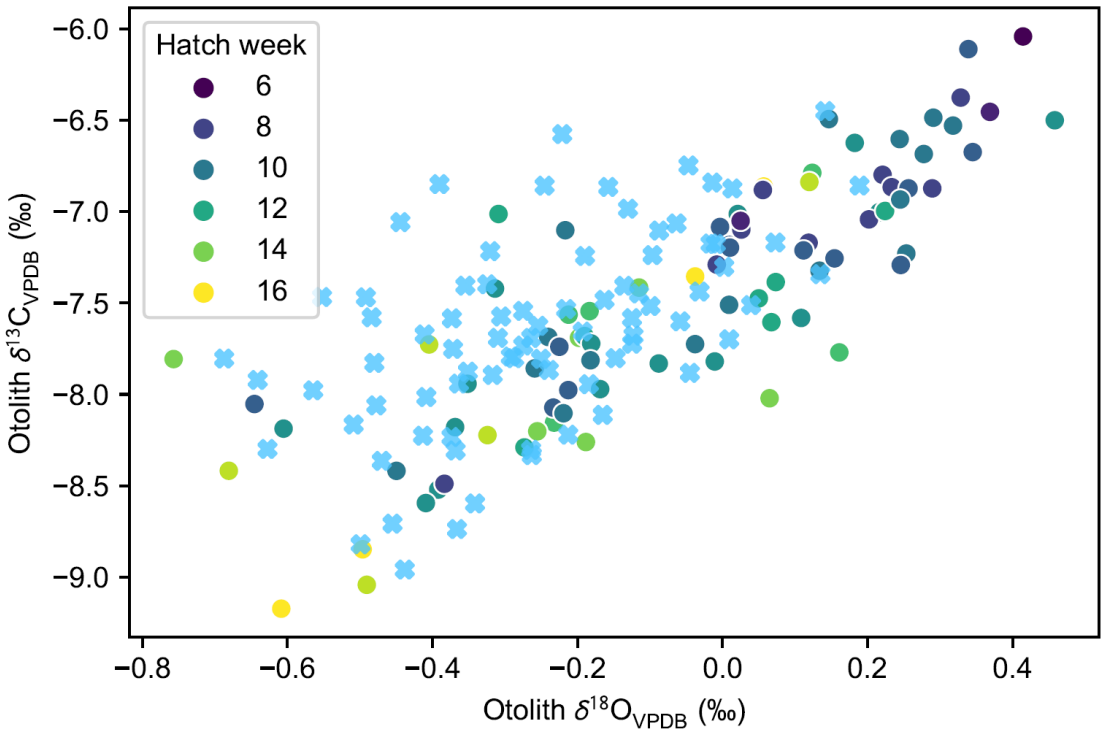

Supplementary Figure S4. Comparison of otolith δ^{18}O and δ^{13}C for spring between the nonlocals (crosses) and the pacific-offshores (circles). The colours of the circles, the pacific-offshores, represent the week of hatch counted from January 1st of each year.

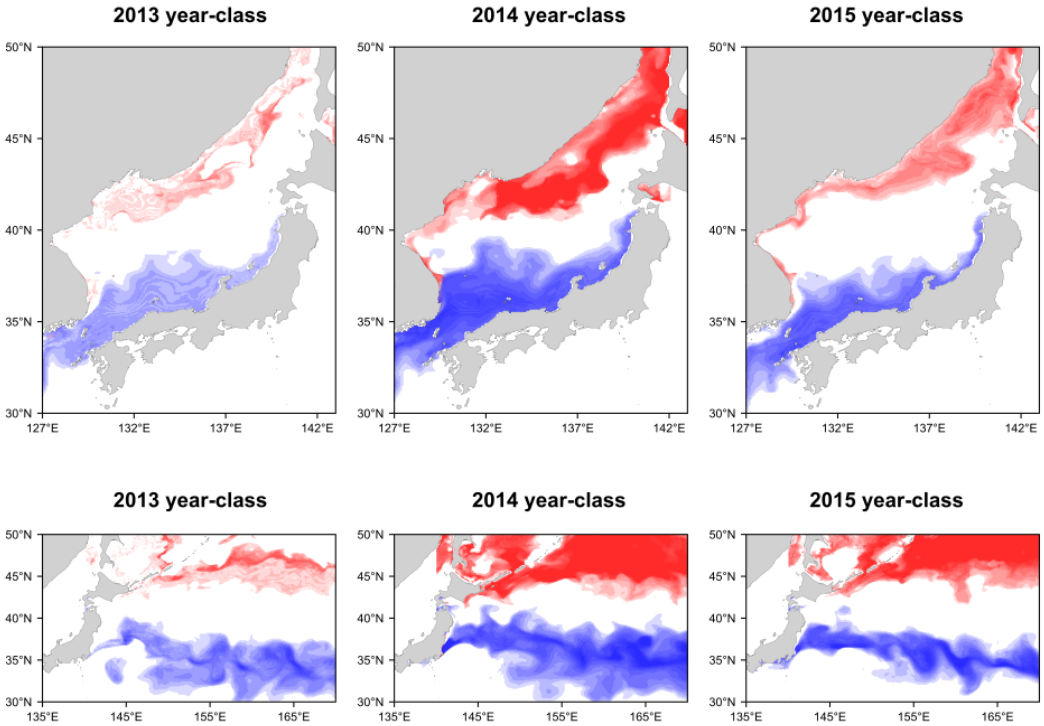

Supplementary Figure S5. Potential distribution of migrants of 2013–2015 year-class during first spring (0–60 dph, blue) and summer (106–120 dph, red) in the Sea of Japan (upper row) and the North Pacific (lower row) predicted based on otolith $\delta^{18}O$ and hydrodynamic models.

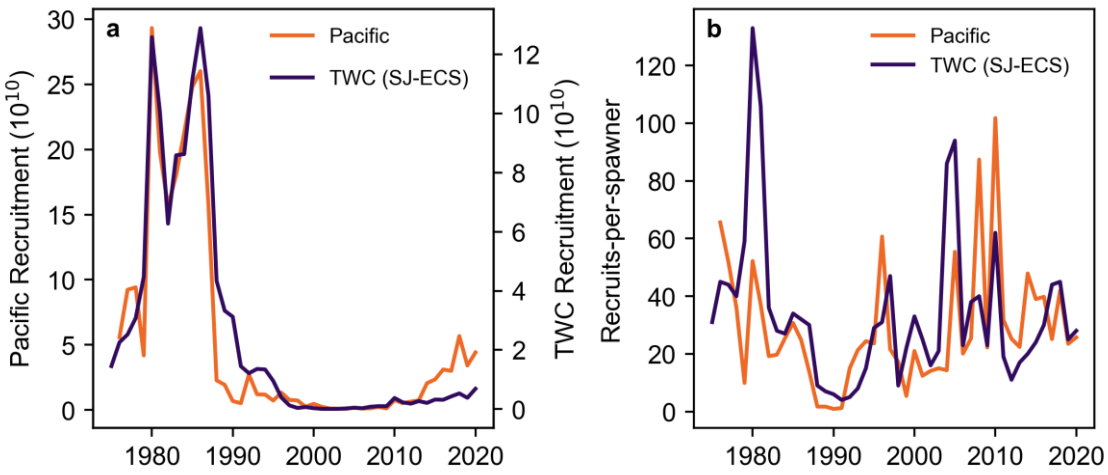

197

198 **Supplementary Figure S6. Time series of recruitment (a) and recruits-per-spawner**
199 **(b) of Pacific (orange) and Tsushima Warm Current (purple) stocks estimated by**
200 **stock assessment models for each.**

201

Supplementary Table S1. Results of pairwise comparisons of spring otolith $\delta^{18}O$ and $\delta^{13}C$ values and otolith radius at 60 dph between the locals, nonlocals and Pacific-offshores based on Games–Howell test.

variables	group1	group2	estimate	p-value (adjusted)
Otolith $\delta^{13}C$	Local	Nonlocal	-0.17	8.5.E-02
Otolith $\delta^{13}C$	Local	Pacific-offshore	0.00	1.0.E+00
Otolith $\delta^{13}C$	Nonlocal	Pacific-offshore	0.17	1.9.E-01
Otolith $\delta^{18}O$	Local	Nonlocal	0.35	**0.0.E+00**
Otolith $\delta^{18}O$	Local	Pacific-offshore	0.54	**9.2.E-14**
Otolith $\delta^{18}O$	Nonlocal	Pacific-offshore	0.19	**7.6.E-06**
Otolith Radius	Local	Nonlocal	50.6	**1.7.E-10**
Otolith Radius	Local	Pacific-offshore	34.2	**6.4.E-05**
Otolith Radius	Nonlocal	Pacific-offshore	-16.4	1.3.E-01

References

Aono, T., Sakamoto, T., Ishimura, T., Takahashi, M., Yasuda, T., Kitajima, S., Nishida, K., Matsuura, T., Ikari, A., Ito, S. (2024) Estimation of migrate histories of the Japanese sardine in the Sea of Japan by combining the microscale stable isotope analysis of otoliths and a data assimilation model. arXiv:2402.18602 (preprint).

Breitenbach, S. F. & Bernasconi S. M. (2011). Carbon and oxygen isotope analysis of small carbonate samples (20 to 100 µg) with a GasBench II preparation device. *Rapid Communications in Mass Spectrometry,* 25, 1910-1914.

Donlon, C. J., Martin, M., Stark, J., Roberts-Jones, J., Fiedler, E., & Wimmer, W. (2012). The operational sea surface temperature and sea ice analysis (OSTIA) system. *Remote Sensing of Environment,* 116, 140-158.

Hirose, N., Takayama, K., Moon, J-H., Watanabe, T., Nishida, T. (2013). Regional data assimilation system extended to the East Asian Marginal Seas. *Umi Sora (Sea and Sky)*, 89, 1–9. doi: info:ndljp/pid/10116140

Igeta, Y., Sassa, C., Takahashi, M., Kuga, M., Kitajima, S., Wagawa, T., Abe, S., Watanabe, C., Setou, T., Nakamura, H. & Hirose, N. (2023). Effect of interannual variations of Kuroshio–Tsushima Warm Current system on the transportation of juvenile Japanese jack mackerel (Trachurus japonicus) to the Pacific coast of Japan. *Fisheries Oceanography,* 32, 133-146.

Ishimura, T., Tsunogai, U., & Gamo, T. (2004). Stable carbon and oxygen isotopic determination of sub-microgram quantities of CaCO3 to analyze individual foraminiferal shells. *Rapid Communications in Mass Spectrometry,* 18, 2883-2888.

Ishimura, T., Tsunogai, U., & Nakagawa, F. (2008). Grain-scale heterogeneities in the stable carbon and oxygen isotopic compositions of the international standard calcite materials (NBS 19, NBS 18, IAEA-CO-1, and IAEA-CO-8). *Rapid Communications in Mass Spectrometry,* 22, 1925-1932.

Kim, S. T., Mucci, A., & Taylor, B. E. (2007). Phosphoric acid fractionation factors for calcite and aragonite between 25 and 75 C: revisited. *Chemical Geology,* 246, 135-146.

Kuroda, H., Setou, T., Kakehi, S., Ito, S.I., Taneda, T., Azumaya, T., Inagake, D., Hiroe, Y., Morinaga, K., Okazaki, M. & Yokota, T., (2017). Recent Advances in Japanese Fisheries Science in the Kuroshio-Oyashio Region through Development of the FRA-ROMS Ocean Forecast System: Overview of the Reproducibility of Reanalysis Products. *Open Journal of Marine Science,* 7, 62.

Nishida, K., & Ishimura, T. (2017). Grain-scale stable carbon and oxygen isotopic variations of the international reference calcite, IAEA-603. *Rapid Communications in Mass Spectrometry,* 31, 1875-1880.

Sakamoto, T., Komatsu, K., Yoneda, M., Ishimura, T., Higuchi, T., Shirai, K., Kamimura, Y., Watanabe, C. & Kawabata, A. (2017). Temperature dependence of δ^{18}O in otolith of juvenile Japanese sardine: Laboratory rearing experiment with micro-scale analysis. *Fisheries Research,* 194, 55-59.

Sakamoto, T., Van Der Lingen, C. D., Shirai, K., Ishimura, T., Geja, Y., Peterson, J., & Komatsu, K. (2020). Otolith δ18O and microstructure analyses provide further evidence of population structure in sardine Sardinops sagax around South Africa. *ICES Journal of Marine Science*, *77*(7-8), 2669-2680.

Sato, K. (2014) Advanced automatic QC Argo Data. *JAMSTEC,* doi:10.17596/0000104

Shirai, K., Koyama, F., Murakami-Sugihara, N., Nanjo, K., Higuchi, T., Kohno, H., Watanabe, Y., Okamoto, K. & Sano, M. (2018). Reconstruction of the salinity history associated with movements of mangrove fishes using otolith oxygen isotopic analysis. *Marine Ecology Progress Series*, 593, 127-139.